Heliyon 6 (2020) e03739

Contents lists available at ScienceDirect

Heliyon

www.elsevier.com/locate/heliyon

Research article

Chimera dynamics in an array of coupled FitzHugh-Nagumo system with shift of close neighbors

Guy Blondeau Soh [a], Patrick Louodop [a], Romanic Kengne [a], Robert Tchitnga [a,b,*]

[a] Laboratory of Electronics, Automation and Signal Processing, Faculty of Science, Department of Physics, University of Dschang, P.O. Box 67 Dschang, Cameroon
[b] Institute of Surface Chemistry and Catalysis, University of Ulm, Albert-Einstein-Allee 47, 89081 Ulm, Germany

ARTICLE INFO

Keywords:
Biophysics
Nonlinear physics
Chimera state
Multi-chimera state
Shift parameter
Step traveling chimera
Neuroplasticity

ABSTRACT

In this paper, we consider an array of FitzHugh-Nagumo (FHN) systems with R close neighbors. Each element (j) connects to another (m) and its $2R$ neighbors. Shifting these neighbors produces particular phenomena such as chimera and multi-chimera. Step traveling chimera is observed for a time dependent shift. Results show that, basing oneself on both shift parameter m and close neighbors R, a full control on the chimera dynamics of the network can be ensured.

1. Introduction

A particular and remarkable spatiotemporal pattern in a ring network of coupled phase oscillators was discovered in 2002 by Kuramoto and Battogtokh [1]. This pattern was characterized by the coexistence of a coherent or synchronized and incoherent or unsynchronized ensemble of oscillators [1]. That behavior, which was called chimera by Abrams and Strogatz in 2004 [2], was later discovered in many systems such as electronic circuits [3, 4, 5, 6, 7], mechanical system [8, 9, 10, 11, 12] chemical systems [13, 14, 15, 16, 17], optical systems [18, 19], and animal world [20]. Some particular patterns of that same behavior have been found such as chimera death states [21, 22], spiral wave chimera [23], multi-chimera [24, 25, 26, 27, 28, 29, 30] and traveling chimera [29, 31, 32, 33]. After its discovery, the chimera state has been investigated in several neuronal processes [29, 34, 35, 36, 37, 38, 39] among which the unihemispheric sleep to explain the sleeping behavior of some animals [20, 40] or migratory birds [20].

The dynamics of arrays of coupled nonlinear oscillators has been a subject of much attention in recent years [41, 42, 43]. In 2017 the authors of [41] found chimera state in an array of coupled oscillators. They show that the discrete Lugiato-Lefever equation supports chimera-like states in an array of coupled-waveguide resonators.

An important topic in applied complex systems science is the control of non-linear systems. Recently, some control techniques, which allow to stabilize chimera patterns in non-locally coupled oscillator networks have been proposed. Among these techniques, we have the tweeter feedback control which can stabilize and fix the position of chimera states [44, 45], the spatial pinning control which can induce a chimera state where the nodes belonging to one domain, either the coherent or the incoherent, are fixed by the control action [46].

Few years ago, some authors such as Changhai Tian et al. [39] or R. Gopal et al. [25] considered the nearest neighbors coupling technics to generate chimera.

Previously, in 2013 the authors of ref. [47] in their investigation on the nearest neighbors coupling technics, defined the rotational coupling matrix to model the cross couplings between activator and inhibitor variables of FitzHugh-Nagumo oscillators. They found that, depending on the coupling strength and range, different multi-chimera states arise in a transition from classical chimera states. In their work, each node j is connected to its R nearest neighbors in each direction namely from $j-R$ to $j+R$. The network topology is fixed and is not time dependent. Each node maintains the same neighbors and the same number of neighbors along the time. This can be seen as a great draw back in case of the description of the dynamics of a class of networks.

* Corresponding author at: Laboratory of Electronics, Automation and Signal Processing, Faculty of Science, Department of Physics, University of Dschang, P.O. Box 67 Dschang, Cameroon.
E-mail address: robert.tchitnga@eaphysud.org (R. Tchitnga).

https://doi.org/10.1016/j.heliyon.2020.e03739
Received 22 December 2019; Received in revised form 20 February 2020; Accepted 31 March 2020

2405-8440/© 2020 Published by Elsevier Ltd. This is an open access article under the CC BY-NC-ND license (http://creativecommons.org/licenses/by-nc-nd/4.0/).

In fact, human brains are plastic, malleable and able to make new pathways. Most of us have very different behaviors and thoughts today than we did 20 years ago. This shift is called neuroplasticity [48, 49]. It is the capacity of neurons and neural networks in the brain to change their connections and behavior in response to new information, sensory stimulation, development, damage, or dysfunction [50, 51, 52].

In this manuscript, we investigate the influence of a new integer parameter that we named shift parameter m on the state of similar oscillators used in [29, 47]. Introducing the shift parameter in non-local coupled oscillators based network gives possibility to have different network configurations along the time. In fact, by applying the shift, each node (j) is not directly connected to its nearest neighbors that is from $j-R$ to $j+R$, but to the nearest neighbors of its corresponding shifted node $j+m$ namely from $j+m-R$ to $j+m+R$. Then whenever the parameter R introduces the nonlocal coupling of the network [29, 33, 34, 39], the parameter m induces the slipping of this nonlocal coupling which is a new process. We found that, for a fixed shift parameter, incoherent regions arise as a function of the values of m. Thus, the number and the mean position of incoherent regions are linked to the parameter m and their widths are function of the number of the considered close neighbors. The random variation of m from one step to another produces multi-chimera with a number of incoherent regions for each step, depending on m. By varying step by step the shift parameter m in time, we are changing the shape of network at each step (the step ΔT of index l is defined as the time duration of one possible configuration of the considered network). Thus step traveling chimera is introduced since a particular dynamics remains only for a considered step and changes for the next one. With our consideration, we have an almost complete control on the dynamics of the network since we can manage the width and the mean position of incoherent region, and can also impose the direction and the speed of the traveling chimera.

The rest of the paper is organized as follows. In Section 2 the network model is presented and how its topology changes at each time step is described. In Section 3, several dynamical behaviors are investigated. Through our simulations it comes out that due to the shift the network can displays chimera, multi chimera, step traveling chimera and so on. At the end of this section, the influence of close neighbors number is investigated. The last section is devoted to the conclusion.

2. Model description

The model in consideration is given by the following set of equations:

$$\begin{cases} b\frac{dx_j}{dt} &= x_j - \frac{x_j^3}{3} - y_j \\ &\quad + \frac{\sigma}{2R(l)} \sum_{k=j+m(l)-R(l)}^{j+m(l)+R(l)} [b_{xx}(x_k - x_j) + b_{xy}(y_k - y_j)] \\ \frac{dy_j}{dt} &= x_j - a + \frac{\sigma}{2R(l)} \sum_{k=j+m(l)-R(l)}^{j+m(l)+R(l)} [b_{yx}(x_k - x_j) + b_{yy}(y_k - y_j)] \end{cases} \quad (1)$$

In this model x_j and y_j are the activator and inhibitor variables, with $1 \le j \le M$, b is a small parameter characterizing the time scale of separation. The system exhibits limit cycle relaxation oscillations for proper choice of the excitability threshold a. The system exhibits either oscillatory behavior for $|a| < 1$ or excitable behavior for $|a| > 1$. σ denotes the coupling parameter. Parameters b_{xx}, b_{xy}, b_{yx}, b_{yy} come from the rotational coupling matrix taken as in [5], defined by:

$$B = \begin{pmatrix} b_{xx} & b_{xy} \\ b_{yx} & b_{yy} \end{pmatrix} = \begin{pmatrix} cos\phi & sin\phi \\ -sin\phi & cos\phi \end{pmatrix} \quad \text{with} \quad \phi \in [-\pi, \pi] \quad (2)$$

For the numerical simulation, we have considered an isolated chain of oscillators. This implies that a signal is null after M nodes and thus the boundary conditions are $(x_k - x_j)$ and $(y_k - y_j)$ for $k < 1$ or when $k > M$.

The present topology differs from the one in [47] not only by the fact that we are dealing with an array but also by the introduction of the shift parameter m ($m = 0, 1, 2, 3, ...M$). R is the number of connected neighbors in each direction, not of the node j ($j = 1, 2, 3, ..., M$) but of the node $j+m$. l ($l = 1, 2, 3, ..., L$) is the index of the step ΔT, where L is the total number of topology changes over time. According to this model and considering $M = 12$, $R = 3$ and $j = 5$, Fig. 1 presents the change of the network topology when the shift parameter is changing as $m = 0$, $m = 3$, $m = 4$ and $m = 5$. This topology changing shows the variation of connections for each value of the parameter m.

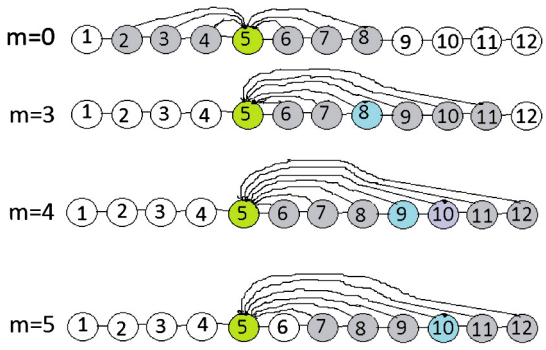

Fig. 1. Changing of network topology for $M = 12$ oscillators with $R = 3$. We select $j = 5$th oscillator and the network is represented for $m = 0$, for $m = 3$, for $m = 4$ and for $m = 5$ from up to down respectively. In the last case, k is supposed to vary from 7 to 13, but connection between $j = 5$ and $j = 13$ does not exist since in this example $M = 12$.

From the model, it comes out that, when $m \le R$, oscillator j is connected to $2R$ neighbors while it is rather linked to $2R+1$ for $m > R$.

3. Dynamical behaviors in the network

In this section, the behavior of the network described by Eq. (1) according to the shift parameter m and the connected neighbors R is investigated. For this investigation, the parameters are fixed at $b = 0.08$, $a = 0.985$, $\phi = \pi/2 - 0.1$, $\sigma = 0.26$, $M = 120$ and the coupled systems are under the initial conditions $x(j) = 0.5 - 0.01j$, $y(j) = 0.047961 - 0.00995j$ for the jth oscillator.

3.1. State for $m = 0$

To better study the influence of the shift parameter m, it is firstly consider a case that there is no shift parameter, namely m is equal to zero. In this case, each considered oscillator is directly connected to its R neighbors in left and right [47]. The space-time plot of the oscillators variables x_j and their corresponding snapshot are given in Fig. 2. It is observed a solitary state in which the position depends on the initial conditions. In this case the most part of the nodes are in stationary state while only the 117th is unsynchronized to the others.

3.2. Shift implies chimera

For fixed values of the shift parameter ($m \neq 0$), the network is in such a way that, each considered oscillator j is not directly connected in each direction to its R nearest neighbors, but to the nearest neighbors of its corresponding shifted oscillator $j+m$. The changing of the network topology from the case $m = 0$ is shown in Fig. 1. The consequence of the introduction of the shift is the fact that chimera occurs and changes depending on the value of m as shown in Fig. 3. By taking $\frac{M}{n+1} \le m \le \frac{M}{n}$, we obtain chimera with n incoherent domains of width $2kR+1$ around the $(M-km)$th oscillator, with $k = 1, 2, 3, ..., n$ respectively. Fig. 3 *a* and *b* show for $n = 1$ ($m = 95$) the presence of one incoherent region depending on the close neighbors around the $(M-m)$th. Fig. 3 *c* and *d* are plotted for $n = 2$ implying ($m = 48$) and $n = 3$ implying ($m = 36$) and present two and three new incoherent regions respectively.

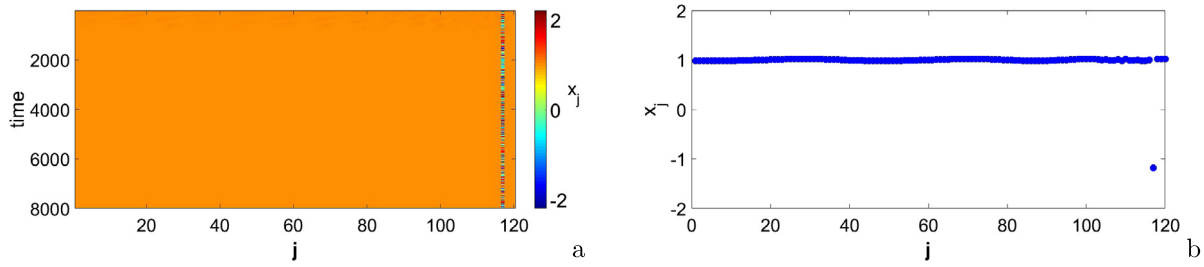

Fig. 2. Dynamics of the nodes for $m = 0$ and $R = 3$. (a) Space-time plot of all nodes variables x_j. (b) Snapshot of variables x_j for 10^5 iterations, a time step of 0.001 and a transient time of 92%.

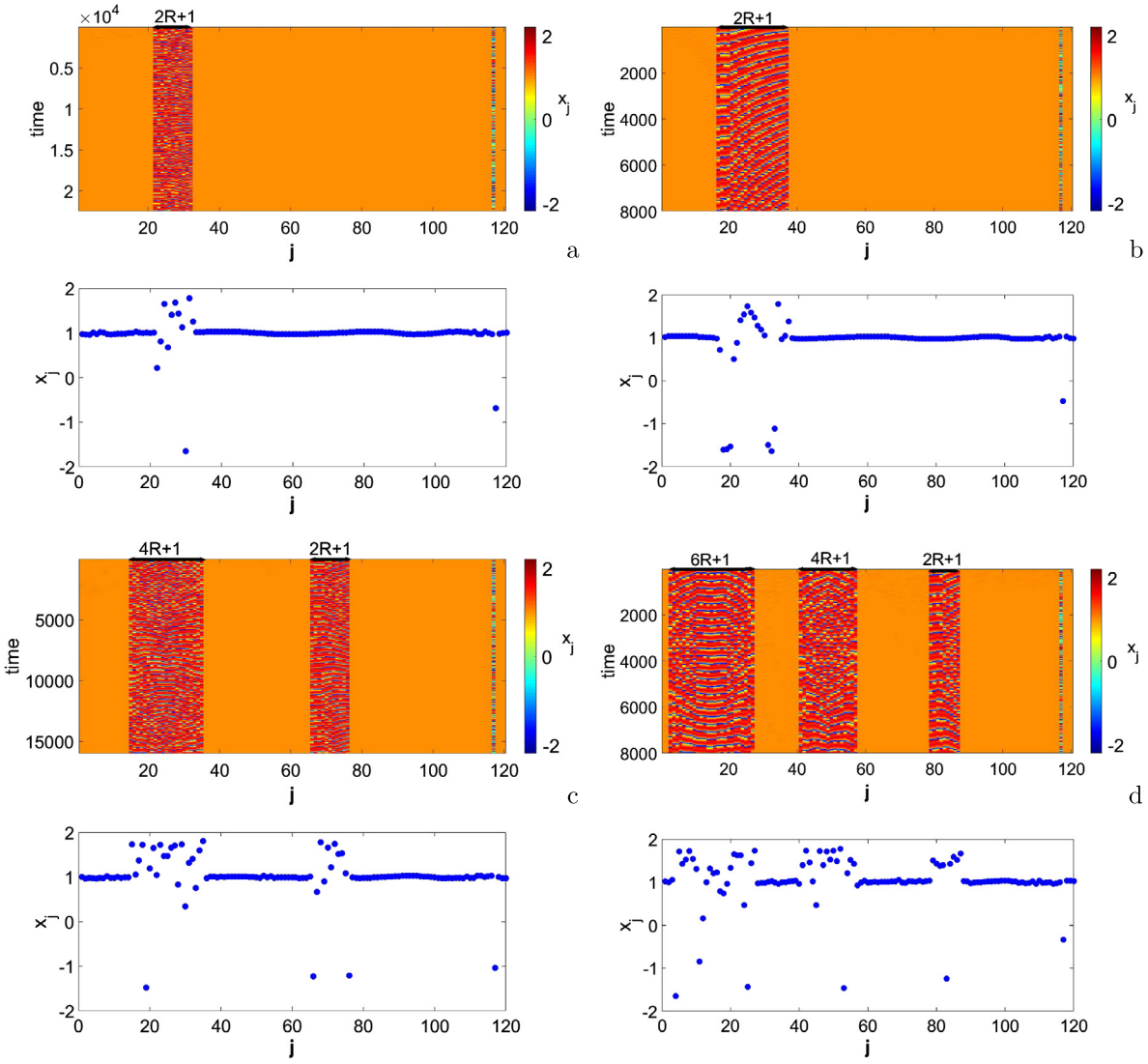

Fig. 3. Chimera state when introducing a shift parameter. Panels present the space-time plot of the oscillators variables x_j and their corresponding snapshot at the stationary states. (a) For $\frac{M}{2} \leq m = 95 \leq \frac{M}{1}$, $R = 5$ it appears one incoherent domain of width $2R + 1 = 11$ around the $(M - m)$th $= 25$th oscillator. (b) For $\frac{M}{2} \leq m = 95 \leq \frac{M}{1}$, $R = 10$ it appears around the $(M - m)$th $= 25$th oscillator one incoherent domain of width $2R + 1 = 21$. (c) For $\frac{M}{3} \leq m = 48 \leq \frac{M}{2}$, $R = 5$ it appears two incoherent domains: the first one of width $2R + 1 = 11$ and the second one of width $4R + 1 = 21$ respectively around the $(M - m)$th $= 72$th and the $(M - 2m)$th $= 24$th oscillator. (d) For $\frac{M}{4} \leq m = 36 \leq \frac{M}{3}$, $R = 4$ it appears three incoherent domains: the first one of width $2R + 1 = 9$, the second one of width $4R + 1 = 17$ and the third one of width $6R + 1 = 25$ respectively around the $(M - m)$th $= 84$th, the $(M - 2m)$th $= 48$th and the $(M - 3m)$th $= 12$th oscillator.

Plotting the time histories of the oscillators in each domain in Fig. 4, a bursting behavior of the nodes is observed in the new incoherent domains (Fig. 4 *c*) as in [33].

From the results in Figs. 3 *a* and *b* where just one major incoherent region was present and in Figs. 3 *c* and *d* where they were respectively two and three major incoherent regions, it is obvious that one can switch from one type to another, that is from the case of one or two incoherent regions to higher number incoherent regions by simply changing the value of the shift parameter m at a certain time as shown in Fig. 5. Figs. 5 *a* and *c* present the switch from two incoherent regions to one, while Figs. 5 *b* and *d* depict the reverse way.

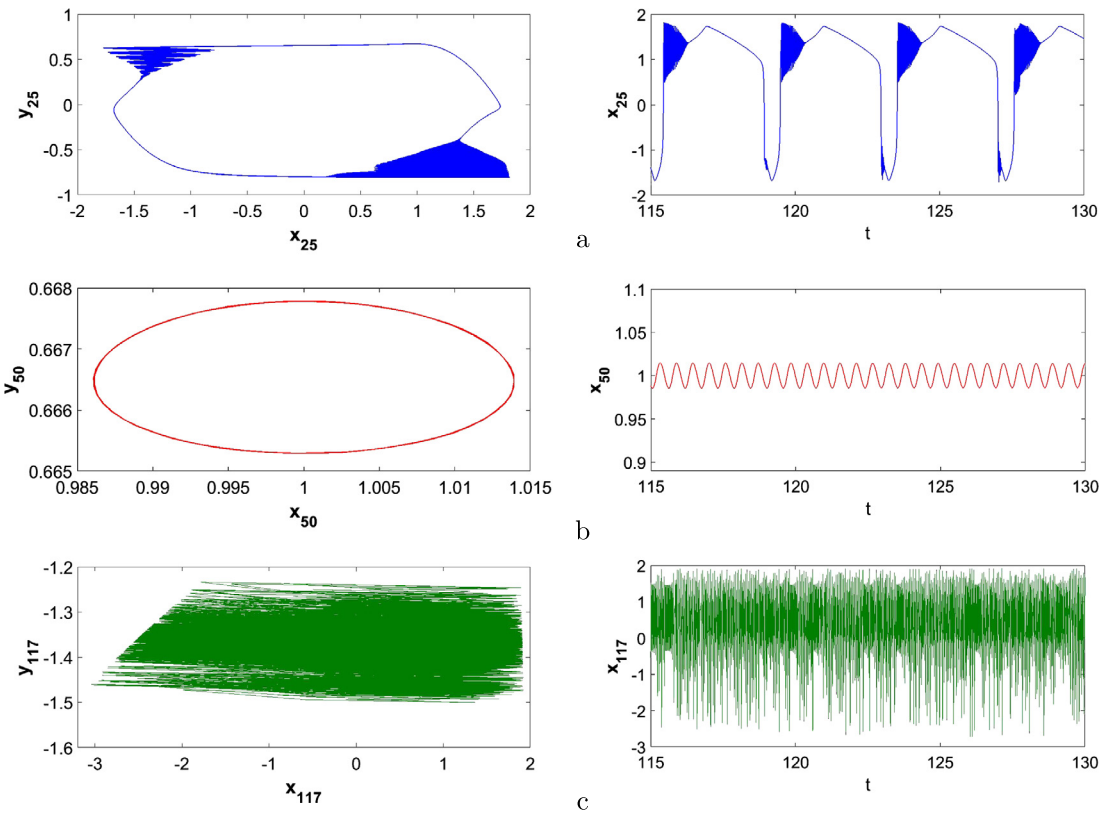

Fig. 4. Time series and phase diagrams of three oscillators (a) $j = 25$, (b) $j = 50$ and (c) $j = 117$ piked out in the incoherent regions ($j = 25, 117$) and coherent region. The network shows coexistence of chaotic bursting, stable behaviors and chaotic oscillation respectively.

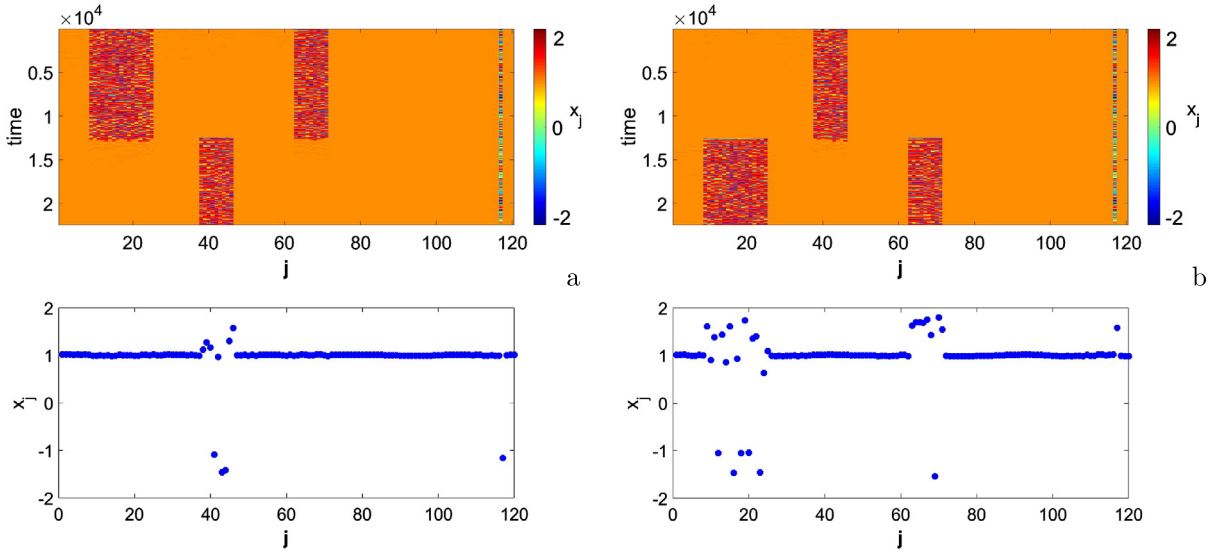

Fig. 5. Change of type of chimera when changing the value of the shift parameter m at a certain time for $R = 5$. (a) Space-time plot of the oscillators variables x_j showing the switch from two to one incoherent regions for the value of m changing from $\frac{M}{2} \leq m = 75 \leq \frac{M}{1}$ to $\frac{M}{3} \leq m = 53 \leq \frac{M}{2}$ and their corresponding snapshot at the stationary states. (b) The space-time plot of the nodes variables x_j showing the switch from one to two incoherent regions for the value of m changing from $\frac{M}{3} \leq m = 53 \leq \frac{M}{2}$ to $\frac{M}{2} \leq m = 75 \leq \frac{M}{1}$ and their corresponding snapshot at the stationary states.

3.3. Effects of stochastic shift parameter and range on the chimera states

Here, it is considered that the total time for numerical simulation is T. T is divided by a chosen number L which is the total number of topologies adopted by the network over time. It is the number of changes in network structure during the period T. Thus, the duration of each configuration which can also be considered as the duration of each step is defined as follows:

$$\Delta T = \frac{T}{L}. \tag{3}$$

In this part, during the period T, we suppose that each configuration or new experience of the network corresponding to the step ΔT occurs randomly by the stochastic variation of m or of R.

The stochastic functions defining evolution of m and R in each step are designed to be integers greater than zero and less than M and $\frac{M}{2}$ respectively. They are given by the following equations:

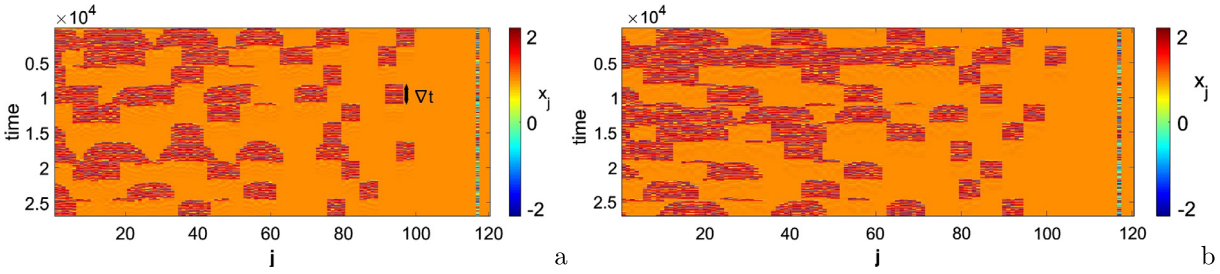

Fig. 6. Step by step change of multi-chimera type when changing randomly the value of the shift parameter m for $R = 2$ and $m_1 = 44$. (a) Space-time plot of the oscillators variables x_j for the first simulation. (b) The space-time plot of the nodes variables x_j for the second simulation.

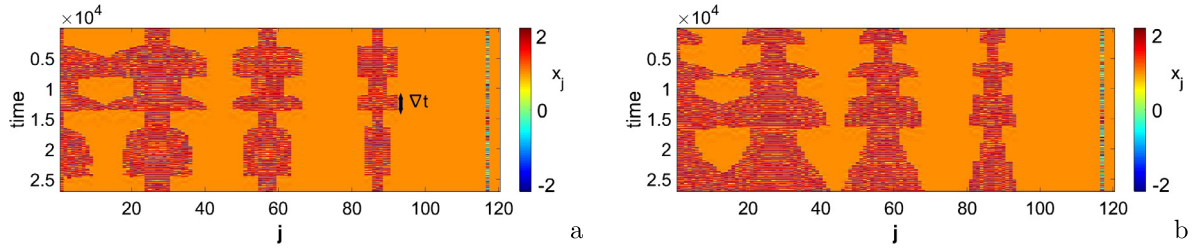

Fig. 7. Step by step change of multi-chimera type when changing randomly the value of the parameter R for $R_1 = 6$ and $m = 32$. (a) Space-time plot of the oscillators variables x_j for the first simulation. (b) The space-time plot of the nodes variables x_j for the second simulation.

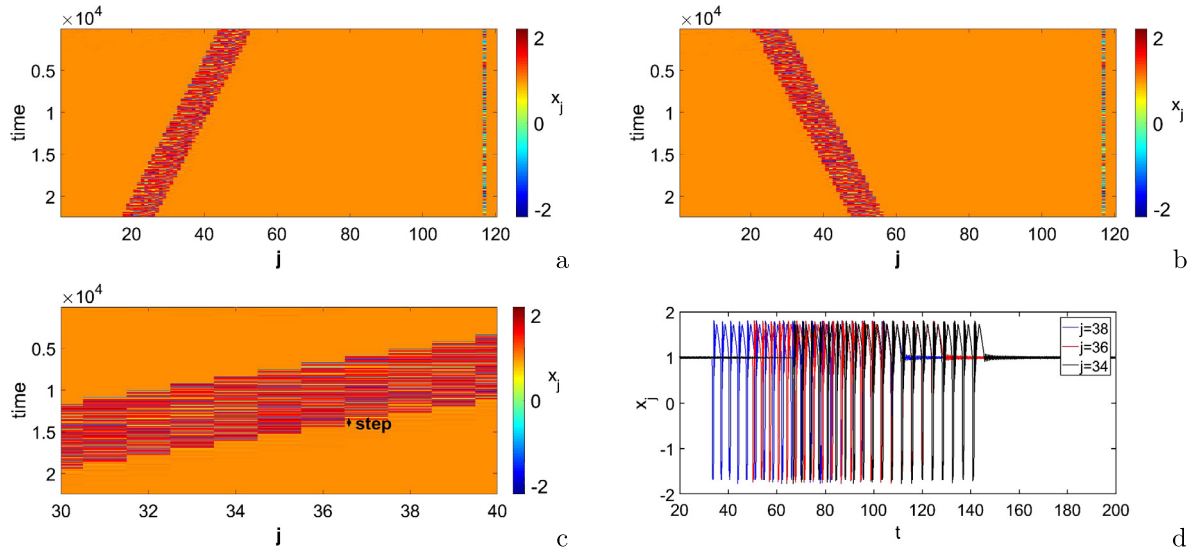

Fig. 8. Step traveling chimera obtained with $R = 5$ and $L = 30$. (a) Left step traveling obtained by increasing $m(l)$ with $p = 1$. (b) Right step traveling obtained by decreasing $m(l)$ with $p = -1$. (c) Enlargement of one small zone of panel (a) confirms the step traveling behavior. (d) Time series of three oscillators $j = 34$, $j = 36$, $j = 38$, exhibiting coherent behavior before and after traveling disorder characterized by the bursting.

$$m(\Delta T) = 1 + round(m_1.rand) \tag{4}$$

$$R(\Delta T) = 1 + round(R_1.rand) \tag{5}$$

Where the function "*rand*" returns random real value between 0 and 1. The expression "$m_1.rand$" returns a random value between 0 and m_1. Since the shift parameter m has to be integer, we used "$round(m_1.rand)$" which provides the nearest integer from "$m_1.rand$". The same analogy is done for "$round(R_1.rand)$". m_1 is taken to be less than M and R_1 is taken to be less than $\frac{M}{2}$.

Figs. 6 and 7 present multi-chimera behavior for two simulations using the same stochastic expressions of m and of R respectively.

Results from Figs. 6 and 7 are always the same as the one of previous subsection namely, by taking $\frac{M}{n+1} \leq m \leq \frac{M}{n}$, we obtain multi-chimera with n incoherent domains of width $2kR + 1$ around the $(M - km)$th oscillator, with $k = 1, 2, 3, ..., n$ respectively. The different is only due to the fact that, in this case, this behavior occurs for each step ΔT and the structure of multi-chimera changes from one step to another depending on the value taken by m.

3.4. Step traveling chimera

m can change progressively by increasing or decreasing step by step. Basing on what has been previously obtained, to have only one new incoherent region, m must be taken between $\frac{M}{2}$ and M. In what follows, the shift parameter changes discretely as a function of the step ΔT represented by its index l according to the following relation:

$$m(\Delta T) = m_0 + p.l \tag{6}$$

where m_0 is the initial value of the shift parameter, p the slope or the speed of incoherent region. The step traveling chimera can be obtained by increasing (right direction as in Fig. 8 *a* with $p > 0$) or decreasing (left direction as in Fig. 8 *b* with $p < 0$) step by step the values of $m(\Delta T)$ be-

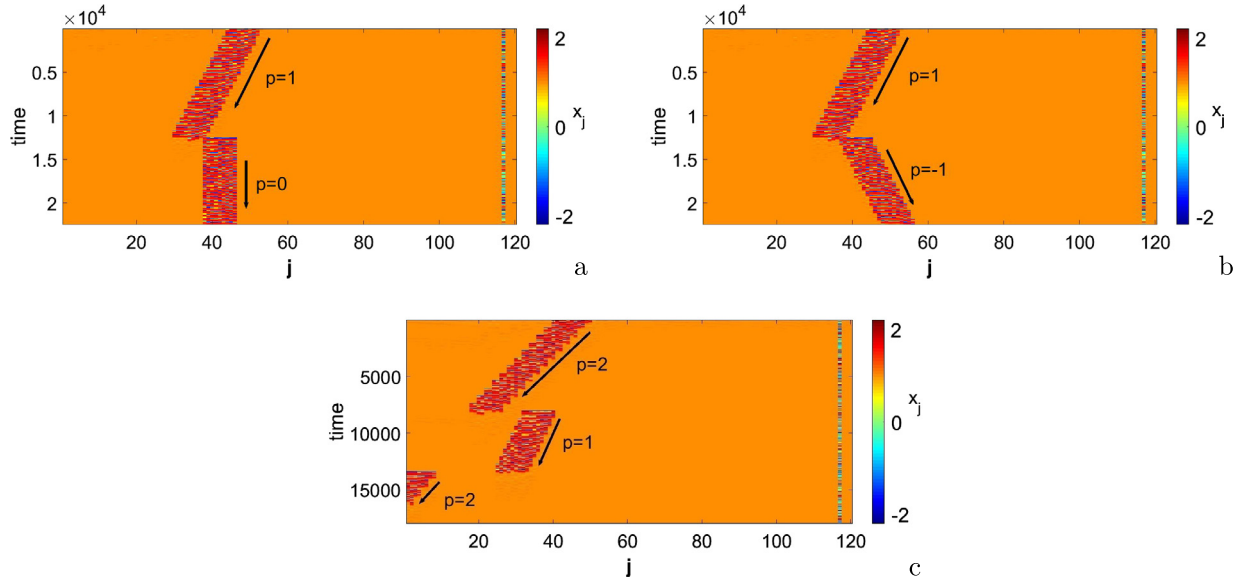

Fig. 9. Broken step traveling chimera obtained when modifying the slope value and/or the sign of the shift parameter with $m_0 = 78$ and $R = 4$. (a) For p stepping from 1 to 0 the step traveling of incoherent subpopulation breaks to become a simple disorder of width $2R+1 = 9$ around the $(M-m)$th $= 42$th. (b) The stepping of p from 1 to -1 changes immediately the direction of the step traveling of the incoherent subpopulation. (c) The changing of speed of the step traveling of incoherent region is induced by the stepping of p firstly from 2 to 1 and secondly from 1 to 2 along the time.

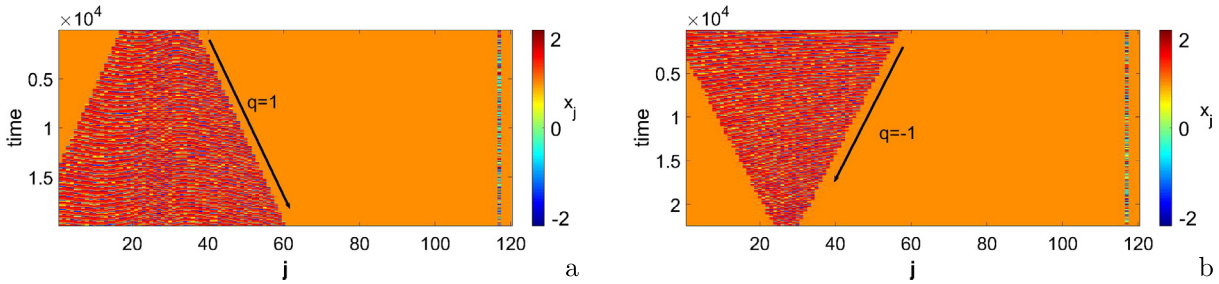

Fig. 10. (a) Propagation step by step of incoherent behavior for $q = 1$. (b) Regression step by step of incoherent behavior for $q = 1$.

tween $M/2$ and M. Fig. 8 *c* shows the time series of $x_j, j = 34, 36, 38$ exhibiting coherent behavior before and after the traveling disorder characterized by a bursting.

By playing with the slope p along the time, it appears that the step traveling chimera can be broken and its direction can be switch depending on slope p in terms of value and sign as shown in Fig. 9.

3.5. *Effect of number of neighbors*

In ref. [47] the author considered a fixed number of neighbors. However, according to the neuroplasticity, the number of neighbors with which a neuron in a brain is coupled changes in time. In our case we consider that the variation of the number of neighbors is done step by step based on the following formula:

$$R(\Delta T) = R_0 + q.l \tag{7}$$

where R_0 is the initial value, q the slope of the straight line and l is the index defining the step of variation of R $(l = 1, 2, 3, ..., L)$. L is the total number of different topologies adopted by the network over time. We observe two different behaviors when we fix $m = 92$ and $L = 30$ according to the value of q. While propagation of incoherent behavior is developed in Fig. 10 *a* by increasing step by step the number of neighbors $(q > 0)$, regression of incoherent behavior is observed in Fig. 10 *b* by decreasing step by step the number of neighbors $(q < 0)$ by step.

4. Conclusion

The main objective of this work was to investigate the dynamic of FitzHugh-Nagumo oscillators in an array for which there is a shift of close neighbors. We found that the shift implied chimera when its value is fixed and can be used to change the nature of the chimera one is dealing with by a simple variation of the shift parameter. In addition of the occurrence of multi-chimera in Fig. 4 of [47], we are presently able to control the widths and positions of incoherent regions through the nearest neighbors number R and the shift parameter m. For a time depending shift parameter, the network displays step by step multi-chimera or a step traveling chimera due to the change of the network topology at each step. Step traveling chimera can be controlled in direction and/or speed or can be broken as shown in Figs. 8 and 9.

Declarations

Author contribution statement

Guy Blondeau Soh: Performed the experiments; Analyzed and interpreted the data; Wrote the paper.

Patrick Louodop: Performed the experiments; Analyzed and interpreted the data.

Romanic Kengne: Performed the experiments.

Robert Tchitnga: Conceived and designed the experiments; Contributed reagents, materials, analysis tools or data; Wrote the paper.

Funding statement

This research did not receive any specific grant from funding agencies in the public, commercial, or not-for-profit sectors.

Competing interest statement

The authors declare no conflict of interest.

Additional information

No additional information is available for this paper.

Acknowledgements

The authors gratefully acknowledge Paul Woafo *(Laboratory of Modeling and Simulation in Engineering, Biomimetics and Prototypes, Faculty of Science, University of Yaound? I, P.O. Box 812, Yaound?, Cameroon)* for very useful discussions and assistance in manuscript preparation.

References

[1] Y. Kuramoto, D. Battogtokh, Coexistence of coherence and incoherence in nonlocally coupled phase oscillators, Nonlinear Phenom. Complex Syst. 5 (2002) 380–385.
[2] D. Abrams, S. Strogatz, Chimera states for coupled oscillators, Phys. Rev. Lett. 93 (2004).
[3] O. Omel'chenko, M. Wolfrum, S. Yanchuk, Y. Maistrenko, O. Sudakov, Stationary patterns of coherence and incoherence in two-dimensional arrays of non-locally-coupled phase oscillators, Phys. Rev. E 85 (2012) 1.
[4] J. Hizanidis, N. Lazarides, G. Neofotistos, G. Tsironis, Chimera states and synchronization in magnetically driven squid metamaterials, Eur. Phys. J. Spec. Top. 225 (2016) 1–5.
[5] A. Vüllings, J. Hizanidis, I. Omelchenko, P. Hövel, Clustered chimera states in systems of type-i excitability, New J. Phys. 16 (2014) 1.
[6] A. Mishra, S. Saha, C. Hens, P. Roy, M. Bose, P. Louodop, H. Cerdeira, S. Dana, Coherent libration to coherent rotational dynamics via chimeralike states and clustering in a Josephson junction array, Phys. Rev. E 95 (2017) 1.
[7] M. Kolahchi, A. Botha, Y. Shukrino, Chimera states in an intrinsically coupled stack of Josephson junctions, J. Supercond. Nov. Magn. 30 (2017) 1659–1663.
[8] A. Slepnev, A. Bukh, T. Vadivasova, Stationary and non-stationary chimeras in an ensemble of chaotic self-sustained oscillators with inertial nonlinearity, Nonlinear Dyn. 88 (2017) 2983–2992.
[9] V. Berec, Explosive synchronization in clustered scale-free networks: revealing the existence of chimera state, Eur. Phys. J. Spec. Top. 225 (2016) 7–15.
[10] Y. Zhu, Z. Zheng, J. Yang, Chimera states on complex networks, Phys. Rev. E 89 (2014) 1.
[11] E. Martens, S. Thutupalli, A. Fourrière, O. Hallatschek, Chimera states in mechanical oscillator networks, Proc. Natl. Acad. Sci. USA 110 (2013) 10563–10567.
[12] T. Kapitaniak, P. Kuzma, J. Wojewoda, K. Czolczynski, Y. Maistrenko, Imperfect chimera states for coupled pendula, Sci. Rep. 4 (2014) 1–10.
[13] M. Tinsley, S. Nkomo, K. Showalter, Chimera and phase-cluster states in populations of coupled chemical oscillators, Nat. Phys. 8 (2012) 662–665.
[14] Y. Kuramoto, D. Battogtokh, H. Nakao, Multiaffine chemical turbulence, Phys. Rev. Lett. 81 (1998) 3543–3546.
[15] A. Hagerstrom, T. Murphy, R. Roy, P. Hövel, I. Omelchenko, E. Schöll, Experimental observation of chimeras in coupled-map lattices, Nat. Phys. (2012) 658–661.
[16] S. Nkomo, M. Tinsley, K. Showalter, Chimera states in populations of nonlocally coupled chemical oscillators, Phys. Rev. Lett. 110 (2013) 1.
[17] M. Wickramasinghe, I. Kiss, Spatially organized dynamical states in chemical oscillator networks: synchronization, dynamical differentiation, and chimera patterns, PLoS ONE 8 (2013) 1–12.
[18] L. Larger, B. Penkovsky, Y. Maistrenko, Laser chimeras as a paradigm for multistable patterns in complex systems, Nat. Commun. 6 (7752) (2015) 1–7.
[19] E. Viktorov, T. Habruseva, S. Hegarty, G. Huyet, B. Kelleher, Coherence and incoherence in an optical comb, Phys. Rev. Lett. 112 (2014) 1.
[20] N. Rattenborg, Do birds sleep in flight?, Naturwissenschaften 93 (2006) 413–425.
[21] A. Zakharova, M. Kapeller, E. Schöll, Amplitude chimeras and chimera death in dynamical networks, J. Phys. Conf. Ser. 727 (2016) 1–11.
[22] P. Dutta, T. Banerjee, Spatial coexistence of synchronized oscillation and death: a chimeralike state, Phys. Rev. E 92 (2015) 1.
[23] J. Totz, J. Rode, M. Tinsley, K. Showalter, H. Engel, Spiral wave chimera states in large populations of coupled chemical oscillators, Nat. Phys. 112 (2017) 1–8.
[24] P. Jaros, L. Borkowski, B. Witkowski, K. Czolczynski, T. Kapitaniak, Multi-headed chimera states in coupled pendula, Eur. Phys. J. Spec. Top. 224 (2015) 1605–1617.
[25] R. Gopal, V. Chandrasekar, A. Venkatesan, M. Lakshmanan, Observation and characterization of chimera states in coupled dynamical systems with nonlocal coupling, Phys. Rev. E 89 (2014) 1.
[26] C. Hens, A. Mishra, P. Roy, A. Sen, S. Dana, Chimera states in a population of identical oscillators under planar cross-coupling, Pramāna 89 (2015) 229–235.
[27] N. Tsigkri-DeSmedt, J. Hizanidis, P. Hövel, A. Provata, Multi-chimera states and transitions in the leaky integrate-and-fire model with nonlocal and hierarchical connectivity, Eur. Phys. J. Spec. Top. 225 (2016) 1149–1164.
[28] P. Hövel, I. Omelchenko, Multi-chimera states in FitzHugh-Nagumo oscillators, BMC Neurosci. 14 (2013) 303.
[29] C. Tian, L. Hongjie, X. Kesheng, L. Zonghua, Chimera states in neuronal networks with time delay and electromagnetic induction, Nonlinear Dyn. 89 (2018) 1–10.
[30] N. Tsigkri-DeSmedt, J. Hizanidis, P. Hövel, A. Provata, Multi-chimera states in the leaky integrate-and-fire model, Proc. Comput. Sci. 66 (2015) 13–22.
[31] J. Xie, E. Knobloch, Multicluster and traveling chimera states in nonlocal phase-coupled oscillators, Phys. Rev. E 90 (2014) 1.
[32] B. Bera, D. Ghosh, T. Banerjee, Imperfect traveling chimera states induced by local synaptic gradient coupling, Phys. Rev. E 94 (2016) 1.
[33] A. Mishra, S. Saha, G. Osipov, S. Dana, Traveling chimera pattern in a neuronal network under local gap junctional and nonlocal chemical synaptic interactions, Oper. Med. Physiol. 3 (2017) 14–18.
[34] D. Dudkowski, Y. Maistrenko, T. Kapitaniak, Different types of chimera states: an interplay between spatial and dynamical chaos, Phys. Rev. E 90 (2014) 1.
[35] J. Hizanidis, N. Kouvaris, G. Zamora-López, A. Díaz-Guilera, C. Antonopoulos, Chimera-like states in modular neural networks, Sci. Rep. 6 (2016) 1–10.
[36] E. Arumugam, M. Spano, A chimeric path to neuronal synchronization, Chaos 25 (2015) 1–5.
[37] S. Majhi, S. Majhi, M. Perc, D. Ghosh, Chimera states in uncoupled neurons induced by a multilayer structure, Sci. Rep. 6 (2016) 1–10.
[38] V. Maksimenko, V. Makarov, B. Bera, D. Ghosh, S. Dana, M. Goremyko, N. Frolov, A. Koronovskii, A. Hramov, Excitation and suppression of chimera states by multiplexing, Phys. Rev. E 94 (2016) 1.
[39] C. Tians, X. Zhang, Z. Wang, Z. Liu, Diversity of chimera-like patterns from a model of 2D arrays of neurons with nonlocal coupling, Front. Phys. 12 (2017) 1–8.
[40] N. Rattenborg, C. Amlaner, S. Lima, Behavioral, neurophysiological and evolutionary perspectives on unihemispheric sleep, Neurosci. Biobehav. Rev. 24 (2000) 817–842.
[41] M. Clerc, M. Ferréand, S. Coulibaly, R. Rojas, M. Tlidi, Chimera-like states in an array of coupled-waveguide resonators, Opt. Lett. 42 (2017) 2906–2909.
[42] F. Kazanci, B. Ermentrout, Pattern formation in an array of oscillators with electrical and chemical coupling, SIAM J. Appl. Math. 67 (2007) 512–529.
[43] N. Rulkov, L. Tsimring, M. Larsen, M. Gabbay, Synchronization and beam forming in an array of repulsively coupled oscillators, Phys. Rev. E 67 (2007) 1.
[44] I. Omelchenko, O. Omelchenko, A. Zakharova, E. Schöll, Optimal design of tweezer control for chimera states, Phys. Rev. E 97 (2018) 1.
[45] I. Omelchenko, T. Hülserand, A. Zakharova, E. Schöll, Control of chimera states in multilayer networks, Front. Appl. Math. Stat. 4 (2019) 1–9.
[46] L. Gambuzza, M. Frasca, Pinning control of chimera states, Phys. Rev. E 94 (2016) 1.
[47] I. Omelchenko, O. Omelchenko, P. Hövel, E. Schöll, When nonlocal coupling between oscillators becomes stronger: patched synchrony or multichimera states, Phys. Rev. Lett. 110 (2013) 1.
[48] M. Mattson, K. Moehl, N. Ghena, M. Schmaedick, A. Cheng, Intermittent metabolic switching, neuroplasticity and brain health, Nat. Rev. Neurosci. 19 (2018) 63–80.
[49] M. Mattson, Glutamate and Neurotrophic Factors in Neuronal Plasticity and Disease, Ann. N.Y. Acad. Sci., vol. 1144, 2008, pp. 97–112.
[50] A. Cheng, Y. Hou, M. Mattson, Mitochondria and neuroplasticity, ASN Neuro 2 (2010) 243–256.
[51] G. Batsikadze, W. Paulus, A. Hasan, J. Grundey, M. Kuo, M. Nitsche, Compromised neuroplasticity in cigarette smokers under nicotine withdrawal is restituted by the nicotinic $\alpha_4\beta_2$-receptor partial agonist varenicline, Sci. Rep. 7 (2017) 1–11.
[52] G. Batsikadze, W. Paulus, A. Hasan, J. Grundey, M. Kuo, M. Nitsche, Neurotrophic factors and neuroplasticity pathways in the pathophysiology and treatment of depression, Psychopharmacology 235 (2018) 2195–2220.